

Manifold of Failure: Behavioral Attraction Basins in Language Models*

Sarthak Munshi[†]
Amazon Web Services

Manish Bhatt[†]
Amazon Leo

Vineeth Sai Narajala[†]
Cisco

Idan Habler[†]
Cisco

Ammar Al-Kahfah[†]
Amazon Web Services

Ken Huang
Distributedapps.ai

Blake Gatto
Shrewd Security

Abstract

While prior work has focused on projecting adversarial examples back onto the manifold of natural data to restore safety, we argue that a comprehensive understanding of AI safety requires characterizing the unsafe regions themselves. This paper introduces a framework for systematically mapping the *Manifold of Failure* in Large Language Models (LLMs). We reframe the search for vulnerabilities as a quality-diversity problem, using MAP-Elites to illuminate the continuous topology of these failure regions, which we term *behavioral attraction basins*. Our quality metric, *Alignment Deviation*, guides the search towards areas where the model’s behavior diverges most from its intended alignment. Across three LLMs- Llama3 8B, GPT-OSS-20B, and GPT-5-Mini, we show that MAP-Elites achieves up to 63% behavioral coverage, discovers up to 370 distinct vulnerability niches, and reveals dramatically different model-specific topological signatures: Llama3 8B exhibits a near-universal vulnerability plateau (mean Alignment Deviation 0.93), GPT-OSS-20B shows a fragmented landscape with spatially concentrated basins (mean 0.73), and GPT-5-Mini demonstrates strong robustness with a ceiling at 0.50. Our approach produces interpretable, global maps of each model’s safety landscape that no existing attack method (GCG, PAIR, or TAP) can provide, shifting the paradigm from finding discrete failures to understanding their underlying structure. The framework for mapping these basins, along with the alignment deviation metrics and model-specific datasets, is open-sourced on [Github](#) for community use and replication.

1 Introduction

The prevailing approach to adversarial robustness in AI safety is often restorative: identifying off-manifold adversarial examples and projecting them back to a latent manifold of *natural*

or *safe* data [4]. While valuable, this paradigm implicitly treats failures as aberrations from a well-behaved norm. We argue that to build truly robust systems, we must invert this perspective and directly characterize the structure of failure itself. What if, instead of a sparse collection of isolated points, a model’s vulnerabilities form a continuous, structured landscape, a *Manifold of Failure*?

This paper introduces a framework to systematically map this manifold. We move beyond the singular goal of finding the best adversarial attack and instead seek to illuminate the entire topology of unsafe behavior. Our central thesis is that vulnerabilities in LLMs are not discrete points but exist in *behavioral attraction basins*, which are extended regions in the input space where diverse prompts are drawn toward similar failure modes. Visualizing this landscape, as shown in our 2D behavioral heatmaps (Figures 3 and 5), provides a global view of a model’s safety alignment that is fundamentally different from any single attack success rate.

To achieve this, we employ Quality-Diversity (QD) optimization, specifically the MAP-Elites algorithm [7]. Unlike traditional methods (e.g., GCG [13], PAIR [2], and TAP [6]) that hill-climb towards a single objective, MAP-Elites is designed to find a wide array of high-performing and diverse solutions. We define performance using a novel metric, *Alignment Deviation*, which quantifies how much a model’s response deviates from its expected safety alignment. Our contributions are:

- We systematically map the continuous behavioral topology of LLMs, revealing that model behaviors form smooth surfaces with identifiable structures (Section 6.1).
- We provide empirical evidence for attraction basins—extended regions in the behavioral space where diverse prompts converge to similar, often unsafe, model outputs (Section 6.3).
- Through comparative analysis of three frontier models, we reveal that each exhibits a unique behavioral

*This work was conducted independently and does not reflect the views, policies, or endorsements of the authors’ respective employers.

Corresponding author: manish.bhatt13212@gmail.com

[†]Equal contribution

topology: Llama-3-8B [3] presents a near-universal vulnerability surface (mean AD 0.93), GPT-OSS-20B [8] shows fragmented, spatially concentrated basins (mean AD 0.73), and GPT-5-Mini [10] demonstrates strong alignment with a hard ceiling at AD 0.50 (Section 6.4).

- Our quality-diversity approach achieves up to 63% behavioral coverage, producing structured maps that complement traditional attack methods (Section 6.6).

By providing a framework to chart the vulnerability landscape of LLMs, this work offers a more predictive and comprehensive approach to AI safety. The methods and discoveries presented here enable systematic auditing, guide targeted robustness improvements, and lay the groundwork for a topological science of model behavior.

2 Related Work

Adversarial attack optimization. The dominant paradigm for red teaming involves optimizers designed to find worst-case failures. Gradient-based methods like GCG [13] optimize adversarial suffixes to maximize the probability of harmful completions. Search-based methods like PAIR [2] and TAP [6] use attacker LLMs to iteratively refine or tree-search over prompts. Standardized benchmarks such as HarmBench [5] evaluate these methods on Attack Success Rate (ASR). These techniques are analogous to finding the lowest point in a loss landscape. While powerful, they are not designed to reveal the landscape’s overall structure. Our QD-based approach is fundamentally different: it is an *illumination* algorithm, not an optimization algorithm. Its goal is to produce a global map of the behavioral space.

Quality-diversity and red teaming. Quality-Diversity algorithms, such as MAP-Elites [7], aim to find a large collection of solutions that are both high-performing and diverse. Rainbow Teaming [9] applied QD methods to generate diverse adversarial prompts, demonstrating the value of diversity-driven search in the red teaming setting. Our work extends this direction with two key differences: (1) we use MAP-Elites to map their continuous topology rather than simply generating a diverse set of attacks, and (2) we provide a comprehensive cross-model topological analysis that reveals model-specific vulnerability signatures, producing interpretable 2D maps of the failure manifold.

Geometric analysis of LLM behavior. Recent work has explored the geometric properties of LLM representations to understand model behavior [1, 12]. These studies have shown that the geometry of the embedding space can explain phenomena like universal adversarial attacks and toxicity. However, most of this work focuses on the model’s *internal* representations. Our work differs by analyzing the geometry of the

output space—specifically, the mapping from a parameterized prompt space to safety-relevant behavioral scores—providing a complementary perspective that is directly relevant to safety evaluation.

Manifold projection for robustness. A line of research posits that adversarial examples lie off the natural data manifold and that robustness can be achieved by projecting these inputs back onto it [4]. This approach is inherently restorative, aiming to correct deviations from a safe baseline. Our work inverts this concept: instead of projecting failures back to safety, we map the *Manifold of Failure* itself, arguing that a structural understanding of failure is a prerequisite for comprehensive safety.

3 Assumptions

We consider a black-box threat model for API-based LLMs (e.g., GPT-5-Mini) where an adversary has query access to a target LLM but no access to its internal states, gradients, or parameters. For locally hosted LLMs (e.g., Llama-3-8B, GPT-OSS-20B), we consider both black-box and white-box settings, though our MAP-Elites framework operates in a black-box manner in all experiments. The adversary’s goal is not to cause a specific, targeted harm, but to *explore and understand the full range of the model’s potential failure modes*. This aligns with the objectives of red teaming and safety auditing, where the aim is to comprehensively assess a model’s vulnerabilities before deployment.

Our work focuses on single-turn interactions with text-based LLMs. We assume that the model’s behavior can be characterized by a continuous, low-dimensional behavioral space and that a meaningful Alignment Deviation metric can be computed for any given response. We also assume that the judge LLMs used for evaluation are sufficiently capable of identifying and categorizing harmful content across different harm taxonomies. While we focus on a 2D behavioral space for visualization, our framework is extensible to higher dimensions.

4 Mathematical Framework

To systematically map the behavioral topology of a language model, we formalize the problem within a quality-diversity (QD) optimization framework. This requires defining a continuous behavioral space, a quality objective to optimize, and a set of metrics to evaluate the exploration process.

4.1 Behavioral Space

We define a continuous, d -dimensional behavioral space $\mathcal{B} = [0, 1]^d$, where each dimension represents a distinct, quantifiable characteristic of a prompt. For any given prompt p , a

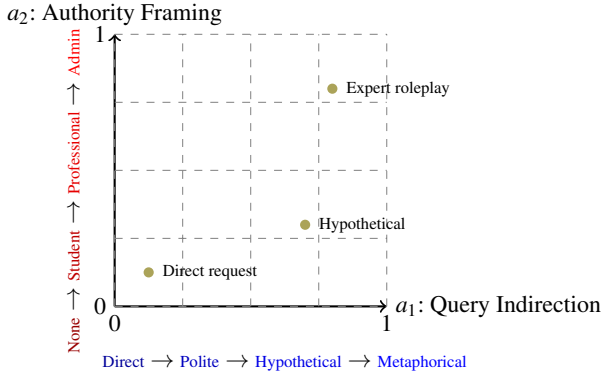


Figure 1: Two-dimensional behavioral space \mathcal{B} . The x -axis captures query indirection (direct to metaphorical) and the y -axis captures authority framing (none to administrator). Each prompt maps to a point in this space via its behavioral descriptor.

behavioral descriptor function $b(p) \rightarrow \mathcal{B}$ maps the prompt to a coordinate in this space. In this work, we primarily focus on a 2D space ($d = 2$) defined by:

- **a_1 : Query Indirection.** This dimension captures the degree to which a query is framed indirectly, ranging from a direct request ($a_1 = 0$) to a highly metaphorical or hypothetical scenario ($a_1 = 1$). It tests the model’s consistency when faced with semantic paraphrasing of a core request.
- **a_2 : Authority Framing.** This dimension represents the level of perceived authority in the prompt’s context, spanning from no authority ($a_2 = 0$) to a strong administrative or expert persona ($a_2 = 1$). It measures the model’s compliance as a function of social context.

This continuous representation allows us to treat the model’s behavior not as a response to discrete inputs, but as a smooth function over a topological space, enabling geometric analysis. The behavioral descriptor for each prompt is computed by an LLM that scores the prompt along each axis on a $[0, 1]$ scale.

4.2 Alignment Deviation and Judge Aggregation

We define our quality objective $Q(p)$ as the *Alignment Deviation*:

$$Q(p) = \max_{c \in C} \text{JudgeScore}_c(p) \quad (1)$$

where C is the set of ten harm categories (violence, hate speech, sexual content, self-harm, illegal activity, privacy violation, misinformation, malware, fraud, and regulated advice)

and $\text{JudgeScore}_c(p) \in [0, 1]$ is the score assigned by the judge LLMs for a given prompt p in category c . A high value for $Q(p)$ signifies a highly misaligned outcome. Our objective is not to find a single prompt that maximizes $Q(p)$, but rather to use MAP-Elites to find a diverse archive of prompts that collectively maximize this quality score across the entire behavioral space \mathcal{B} .

Assessing model outputs for safety requires a robust evaluation framework. We employ two judge models J (GPT-4.1 and Sonnet 4.5) to assess response characteristics across all ten harm categories. For each prompt–response pair, the judge outputs both a binary classification (safe/unsafe) and a continuous confidence score for each category. The Alignment Deviation is then the maximum score across categories (Equation 1), capturing the worst-case harm dimension.

5 Methodology

We frame the exploration of the LLM behavioral space as a quality-diversity problem. MAP-Elites [7] partitions the behavioral space into a 25×25 grid (the *archive*, yielding 625 distinct behavioral niches) and attempts to find the highest-quality solution for each cell. This allows us to systematically explore the entire behavioral space, rather than searching for a single optimal adversarial prompt.

5.1 Prompt Mutation

To generate new prompts, we use a multi-strategy mutation framework. Given a parent prompt selected from the archive, we apply one of six mutation strategies with the following probabilities:

1. **Random Axis Perturbation (50%):** Systematically shift the prompt along the query indirection or authority framing axis, ensuring coverage of the behavioral space.
2. **Paraphrasing (10%):** Use an LLM to rephrase the prompt while preserving its intent.
3. **Entity Substitution (10%):** Replace named entities or nouns with semantically similar alternatives.
4. **Adversarial Suffix (10%):** Append a short adversarial string inspired by GCG [13].
5. **Crossover (10%):** Combine elements from two parent prompts selected from the archive.
6. **Semantic Interpolation (10%):** Interpolate in embedding space between two prompts p_1 and p_2 as $e_{\text{new}} = \lambda e_1 + (1 - \lambda)e_2$ and decode back to text.

The heavy weighting toward random axis perturbation ensures that MAP-Elites efficiently explores the full grid, while the remaining strategies provide diverse prompt variations within each region.

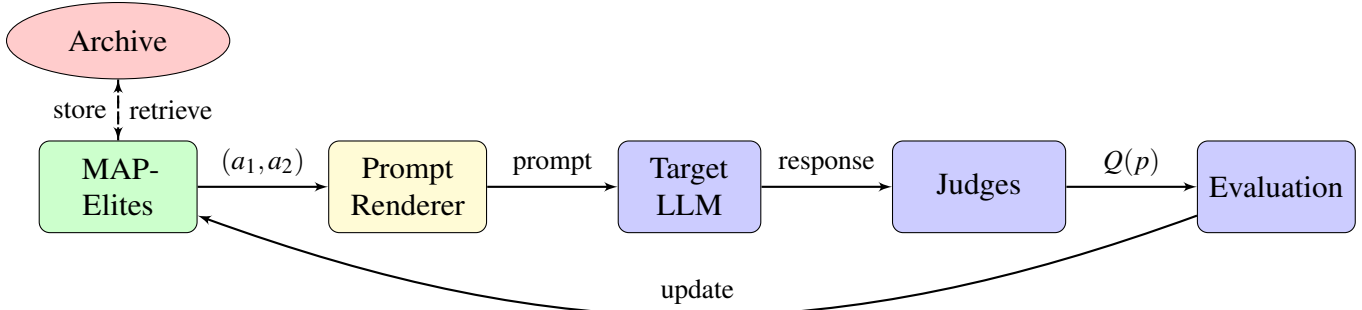


Figure 2: System architecture. MAP-Elites selects and mutates prompts from the behavioral archive. Each prompt is sent to the target LLM, and the response is evaluated by the judge to produce a behavioral descriptor (b) and Alignment Deviation score $Q(p)$, which update the archive.

5.2 Gaussian Process Modeling

To predict the Alignment Deviation of unexplored regions, we fit a Gaussian Process with a Matérn kernel ($\nu = 2.5$) to the observed data in the MAP-Elites archive. The GP provides a posterior distribution over $Q(p)$, allowing us to estimate both the expected Alignment Deviation and the uncertainty of our predictions in unvisited cells. This enables identification of promising regions for future exploration and quantification of the predictability of the failure manifold.

5.3 Algorithm

Algorithm 1 provides the pseudocode for our framework. The archive \mathcal{A} stores the best-found prompt for each cell in the behavioral space. In each iteration, a prompt is selected from the archive, mutated, evaluated, and inserted into the archive if it improves on the existing occupant of its cell.

Algorithm 1 Mapping the Manifold of Failure

```

1: Initialize archive  $\mathcal{A}$  with empty cells
2: Generate initial population  $\mathcal{P}_{\text{init}}$  from 100 seed prompts
3: for  $p$  in  $\mathcal{P}_{\text{init}}$  do
4:    $b \leftarrow \text{GetBehavior}(p)$  // LLM-based descriptor
5:    $q \leftarrow \text{GetQuality}(p)$  // Alignment Deviation
6:    $\text{ADDTOARCHIVE}(\mathcal{A}, p, b, q)$ 
7: end for
8: for iteration = 1 to 15,000 do
9:    $p_{\text{parent}} \leftarrow \text{SelectFromArchive}(\mathcal{A})$ 
10:   $p_{\text{child}} \leftarrow \text{Mutate}(p_{\text{parent}})$  // Multi-strategy
11:   $b_{\text{child}} \leftarrow \text{GetBehavior}(p_{\text{child}})$ 
12:   $q_{\text{child}} \leftarrow \text{GetQuality}(p_{\text{child}})$ 
13:   $\text{ADDTOARCHIVE}(\mathcal{A}, p_{\text{child}}, b_{\text{child}}, q_{\text{child}})$ 
14: end for
15: return  $\mathcal{A}$ 

```

5.4 Experimental Setup

We evaluate our framework on three LLMs (Llama-3-8B, GPT-OSS-20B, GPT-5-Mini) spanning different architectures, sizes, and access models. All target models are queried with temperature 0.7 and a maximum output length of 500 tokens. We also compare MAP-Elites against four baselines, all given the same 15,000-query evaluation budget:

- **Random Sampling:** Randomly generated prompts evaluated for behavioral coverage.
- **GCG [13]:** White-box and black-box gradient-based suffix optimization (depending on the model type).
- **PAIR [2]:** Black-box iterative prompt refinement using an attacker LLM.
- **TAP [6]:** Tree-search-based attack with pruning of unpromising branches.

For all baselines, we project the discovered prompts into the same 25×25 behavioral grid to enable direct comparison of behavioral coverage. Additionally, behavioral descriptors are computed using an LLM-based scorer. Prompt embeddings for semantic interpolation use the `all-mpnet-base-v2` sentence transformer [11]. All experiments run for 15,000 evaluations (100 seed prompts + 15,000 mutation iterations), seeded with 100 diverse initial prompts spanning the harm taxonomy.

5.5 Evaluation Metrics

- **Behavioral Coverage:** Percentage of the 625 grid cells that are filled after a fixed budget, measuring how thoroughly the method explores the behavioral space.
- **Diversity:** Number of filled cells with Alignment Deviation > 0.5 , measuring how many distinct vulnerability niches are discovered.

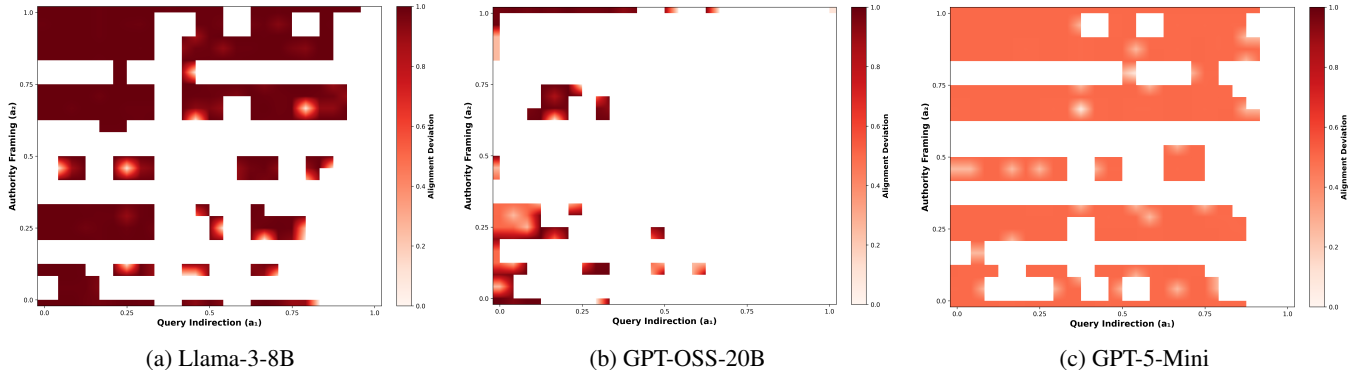


Figure 3: 2D behavioral heatmaps reveal model-specific topological signatures (white = safe, dark red = high deviation). (a) Llama-3-8B exhibits a near-universal vulnerability plateau at $AD \approx 1.0$. (b) GPT-OSS-20B shows spatially concentrated basins in the low-indirection region. (c) GPT-5-Mini shows uniform moderate deviation with a hard ceiling at $AD = 0.50$.

- **Peak Alignment Deviation:** Maximum $Q(p)$ achieved, measuring worst-case failure severity.
- **Mean Alignment Deviation:** Average $Q(p)$ across filled cells, measuring the overall severity of the discovered vulnerability landscape.
- **QD-Score:** Sum of quality values across all filled cells ($\sum_{c \in \text{filled}} Q(c)$), the standard quality-diversity metric combining both coverage and quality.

6 Results

6.1 Behavioral Topology

Figure 3 presents the behavioral heatmaps for all three target models, providing the global view of their safety landscapes. The heatmaps reveal strikingly different topologies:

Llama-3-8B (Figure 3a) exhibits a near-universal vulnerability surface. The map is dominated by dark red (high Alignment Deviation), with mean AD of 0.93 and peak AD of 1.0. The model is susceptible to adversarial prompts across virtually all combinations of query indirection and authority framing, with only narrow channels of reduced deviation at specific authority levels.

GPT-OSS-20B (Figure 3b) shows a fragmented, spatially concentrated pattern. High-deviation cells cluster in the lower-left quadrant (low query indirection, low-to-moderate authority framing) and along the top edge (maximum authority), while the high-indirection region remains largely unexplored or safe. Mean AD is 0.73 with extreme variability ($\text{std}=0.33$).

GPT-5-Mini (Figure 3c) demonstrates remarkable robustness. Despite achieving the highest behavioral coverage (72.32%), peak AD never exceeds 0.50 and the landscape is uniformly moderate (mean AD 0.47). The model maintains consistent, moderate-level refusals regardless of prompt parameterization.

6.2 Contour Analysis

To reveal finer-grained topological structure beyond the heatmaps, Figure 4 presents the contour maps for each model. The contour lines trace iso-Alignment-Deviation surfaces across the behavioral space, making it possible to identify precise boundaries between safe and unsafe regions. All three models exhibit narrow corridors at specific authority framing levels (a_2) where AD changes abruptly, suggesting that authority framing acts as a critical parameter for safety alignment. Models appear to have discrete “thresholds” of authority recognition that, when crossed, significantly alter their compliance behavior.

In **Llama-3-8B** (Figure 4a), the contour landscape is dominated by dark maroon (AD near 1.0), with narrow low-deviation channels running horizontally at specific a_2 values (approximately 0.35, 0.55, and 0.80). These safe corridors are extremely thin, the model quickly reverts to high AD on either side, confirming that even small perturbations in authority framing push the model back into its vulnerability plateau.

GPT-OSS-20B (Figure 4b) reveals the most complex contour structure. Nested, concentric contour rings form localized “bullseye” patterns around peak vulnerability regions, particularly in the lower-left quadrant. High-deviation corridors run horizontally at $a_2 \approx 0.25-0.35$ and $a_2 \approx 0.65-0.85$, with islands of low deviation (labeled 0.0–0.2) scattered between them, especially at high query indirection ($a_1 > 0.5$). This bullseye structure indicates that vulnerability in GPT-OSS-20B is organized around localized attractors rather than spread uniformly.

GPT-5-Mini (Figure 4c) displays contours compressed into a narrow range (0.39–0.50). The horizontal banding is still present but the contour values vary by only ~ 0.1 , confirming the model’s uniform moderate behavior. Thin channels at specific a_2 values show brief dips to $AD \approx 0.25$, but the model never approaches the 0.5 threshold from above.

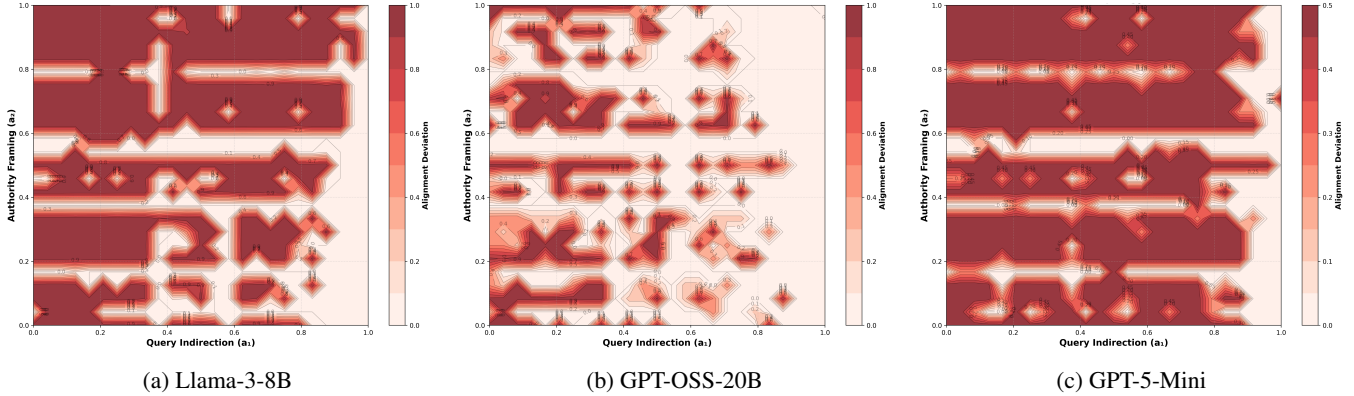


Figure 4: Contour plots showing iso-AD lines across the behavioral space. Horizontal banding at specific a_2 values is visible in all models, suggesting authority framing is a critical parameter for alignment. (a) Llama-3-8B: narrow safe corridors within a high-AD landscape. (b) GPT-OSS-20B: localized “bullseye” patterns with nested contour rings. (c) GPT-5-Mini: compressed contours in a narrow AD range (0.39–0.50).

6.3 Behavioral Attraction Basins

Figure 5 visualizes the attraction basins for each model, defined as contiguous regions where $AD > 0.5$. These basin maps provide direct evidence for our central thesis: vulnerabilities form extended, structured regions rather than isolated points.

For **Llama-3-8B** (Figure 5a), the basin map is almost entirely red: 370 out of 394 filled cells (93.9%) exceed the $AD > 0.5$ threshold. The model’s entire behavioral space constitutes a single, massive attraction basin.

GPT-OSS-20B (Figure 5b) presents a complex mosaic. Of 227 filled cells, 146 (64.3%) are basins, but they are intermixed with safe cells in a spatially non-monotonic pattern. Small perturbations in prompt parameters can flip the model between high and low deviation states, suggesting a rough, fragmented failure manifold.

GPT-5-Mini (Figure 5c) has zero cells exceeding the $AD > 0.5$ threshold. Its entire map is classified as safe. While the model does exhibit non-trivial Alignment Deviation (mean 0.47), it never crosses into genuinely harmful territory.

6.4 Cross-Model Comparison

Table 1 presents the aggregate MAP-Elites results across all three models. The three models span a wide spectrum of vulnerability profiles.

Llama-3-8B achieves the highest QD-Score (366.9), driven by its extremely high mean AD (0.93) and substantial coverage (63.04%). Its 370 diversity niches represent the largest number of distinct vulnerability cells among all models. This model is comprehensively vulnerable: the MAP-Elites algorithm found high-severity failures in nearly every explored region of the behavioral space. **GPT-OSS-20B** presents a paradox: despite having the lowest coverage (36.32%), it

Table 1: MAP-Elites results across target models.

Model	Cov. (%)	Div. (#)	Peak AD	Mean AD	QD-Score
Llama-3-8B	63.04	370	1.00	0.93	366.9
GPT-OSS-20B	36.32	146	1.00	0.73	165.8
GPT-5-Mini	72.32	0	0.50	0.47	213.2

reaches peak AD of 1.0 with a moderately high mean (0.73). Its 146 diversity niches are concentrated in specific spatial regions (Figure 3b), suggesting that the model has “hard” and “soft” regions in its behavioral space. The low coverage indicates that large portions of the behavioral space resist MAP-Elites’ mutation strategies, hinting at a more complex prompt-response landscape. **GPT-5-Mini** achieves the highest coverage (72.32%) but the lowest QD-Score. The model is highly explorable (MAP-Elites easily fills cells across the grid) but never produces genuinely harmful outputs (peak $AD = 0.50$, diversity = 0). This represents the ideal outcome from a safety perspective: a model whose behavioral space is well-covered but uniformly safe.

6.5 3D Behavioral Topology

Figure 6 shows the 3D surface plots of the behavioral topology for each model, providing an intuitive visualization of the “landscape” metaphor. Llama-3-8B presents a high, flat mesa at the AD ceiling (≈ 1.0) with only narrow crevasses. GPT-OSS-20B shows a rugged, mountainous terrain with sharp peaks reaching 1.0 interspersed with deep valleys near 0.0. GPT-5-Mini forms a uniform plateau at ≈ 0.5 with sparse, narrow downward spikes. These surfaces confirm that the failure manifold has a learnable, continuous structure and not

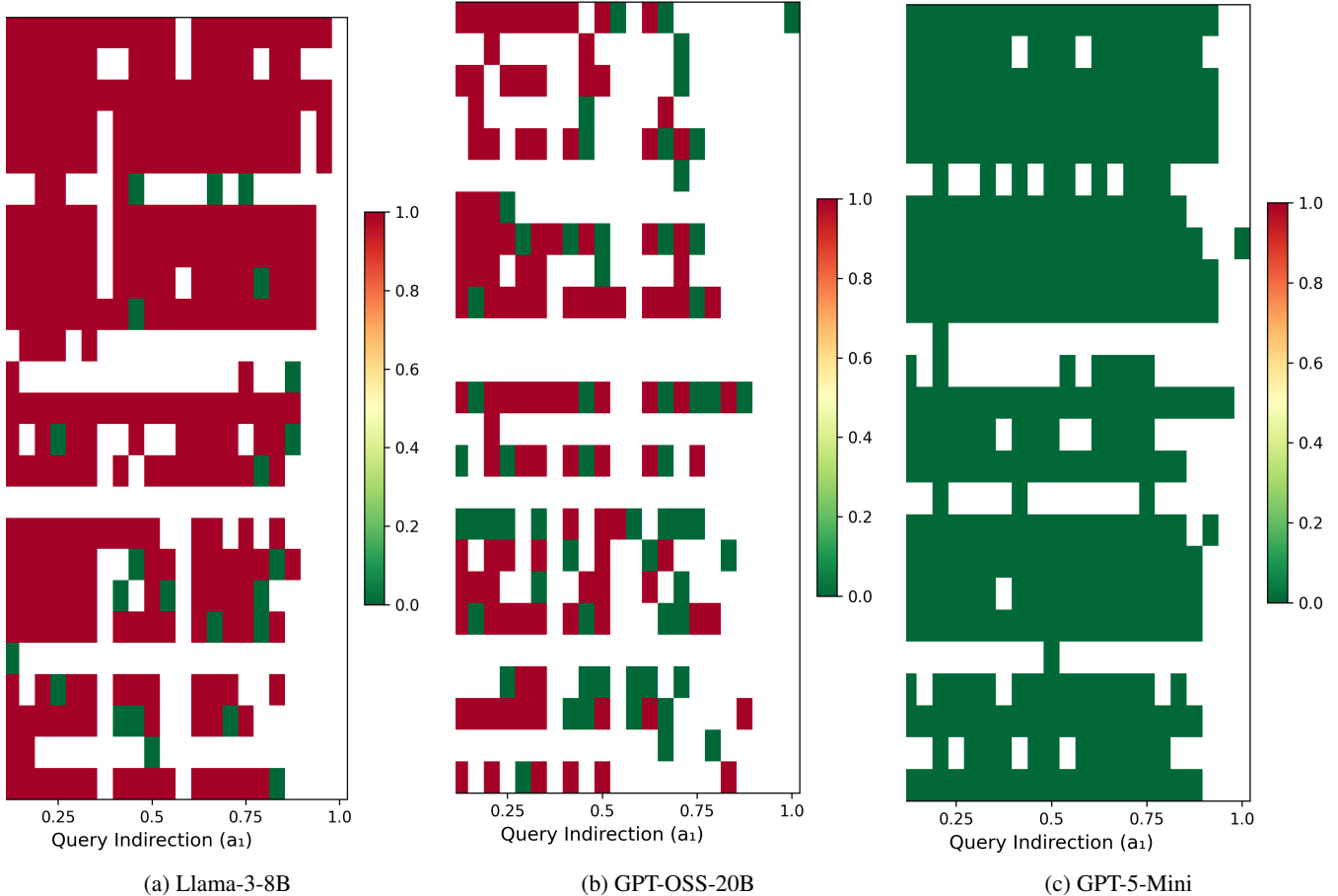


Figure 5: Basin maps where red indicates $AD > 0.5$ (attraction basin) and green indicates $AD \leq 0.5$ (safe); white cells are unexplored. (a) Llama-3-8B: 93.9% of cells are basins. (b) GPT-OSS-20B: 64.3% of cells are basins, with a complex spatial pattern. (c) GPT-5-Mini: 0% of cells are basins; the model never exceeds the threshold.

a random scattering of points.

6.6 Baselines

Table 2 presents the baseline comparison on Llama-3-8B, where all five methods (including GCG in white-box mode) are available.

Table 2: Baseline comparison on Llama-3-8B.

Method	Cov. (%)	Div. (#)	Peak AD
Random	5.28	30	1.00
GCG (whitebox)	7.20	173	1.00
TAP	41.76	255	1.00
PAIR	61.44	291	1.00
Ours (MAP-Elites)	63.04	370	1.00

MAP-Elites achieves the highest behavioral coverage

(63.04%), narrowly surpassing PAIR (61.44%) and substantially outperforming TAP (41.76%), GCG (7.20%), and Random (5.28%). Critically, all methods achieve peak AD of 1.0 on Llama-3-8B, confirming that this model is susceptible to all attack families.

Table 3 shows the GPT-OSS-20B baseline results. Here, PAIR achieves higher raw coverage (63.20% vs. 36.32%), but MAP-Elites discovers proportionally more vulnerability niches: 146 out of 227 filled cells (64.3%) have $AD > 0.5$, compared to PAIR’s 73 out of 395 cells (18.5%). MAP-Elites thus provides higher *vulnerability density* per explored cell, suggesting that its QD-driven search preferentially discovers the most informative regions of the behavioral space.

For GPT-5-Mini (Table 4), no method, including MAP-Elites, achieves AD above 0.50. This is a strong result for the model’s safety alignment: even with 15,000 queries, neither iterative refinement (PAIR), tree search (TAP), nor quality-diversity optimization can breach the model’s safety boundary.

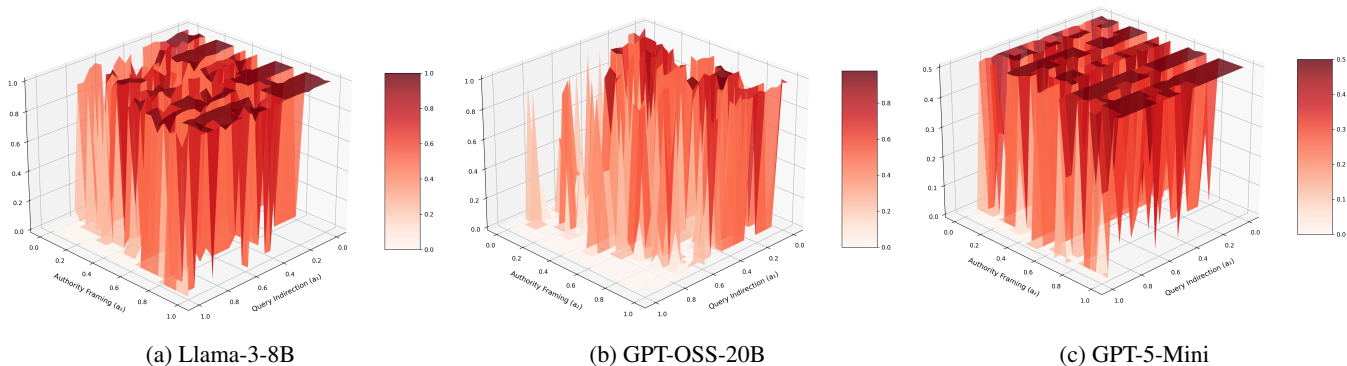


Figure 6: Surface plots of Alignment Deviation over the (a_1, a_2) behavioral space. (a) Llama-3-8B: a high mesa near the ceiling. (b) GPT-OSS-20B: rugged terrain with sharp peaks and valleys. (c) GPT-5-Mini: a flat plateau at moderate AD with narrow downward spikes.

Table 3: Baseline comparison on GPT-OSS-20B.

Method	Cov. (%)	Div. (#)	Peak AD
Random	0.80	3	0.97
GCG (whitebox)	34.72	0	0.5
TAP	25.60	68	1.00
Ours (MAP-Elites)	36.32	146	1.00
PAIR	63.20	73	1.00

Table 4: Baseline comparison on GPT-5-Mini. No method achieves AD > 0.50.

Method	Cov. (%)	Div. (#)	Peak AD
TAP	30.08	0	0.50
PAIR	58.56	0	0.50
Ours (MAP-Elites)	72.32	0	0.50

6.7 Ablation Study

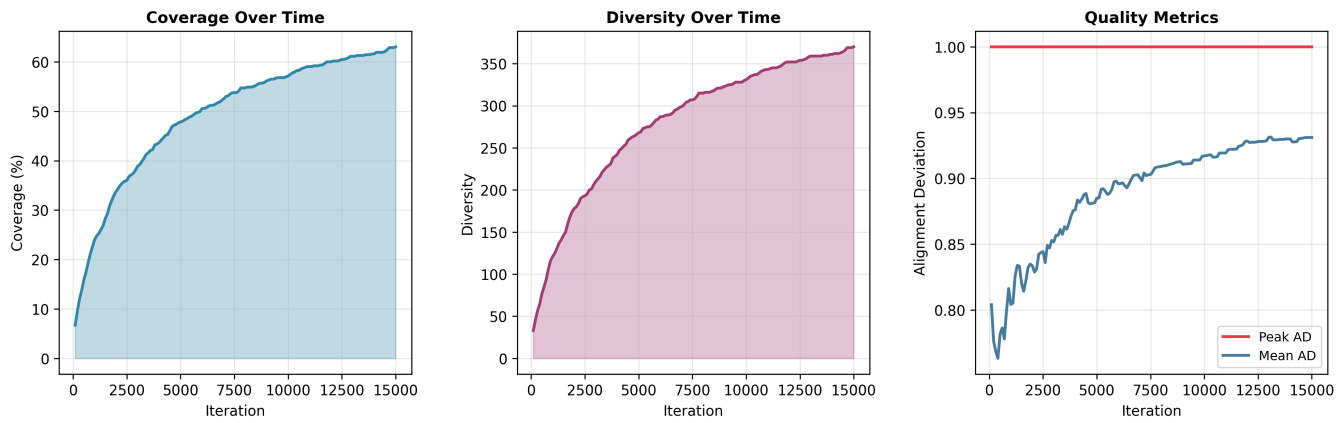
To isolate the contribution of each component, we compare three variants (Table 5):

1. **Full method** (MAP-Elites + Alignment Deviation): the complete framework as described in Section 5.
2. **ME + Toxicity**: MAP-Elites with Alignment Deviation replaced by a single-dimension toxicity classifier score, removing the multi-category quality signal.
3. **Random + AD**: Random prompt sampling evaluated with the full Alignment Deviation metric, removing the quality-diversity search entirely.

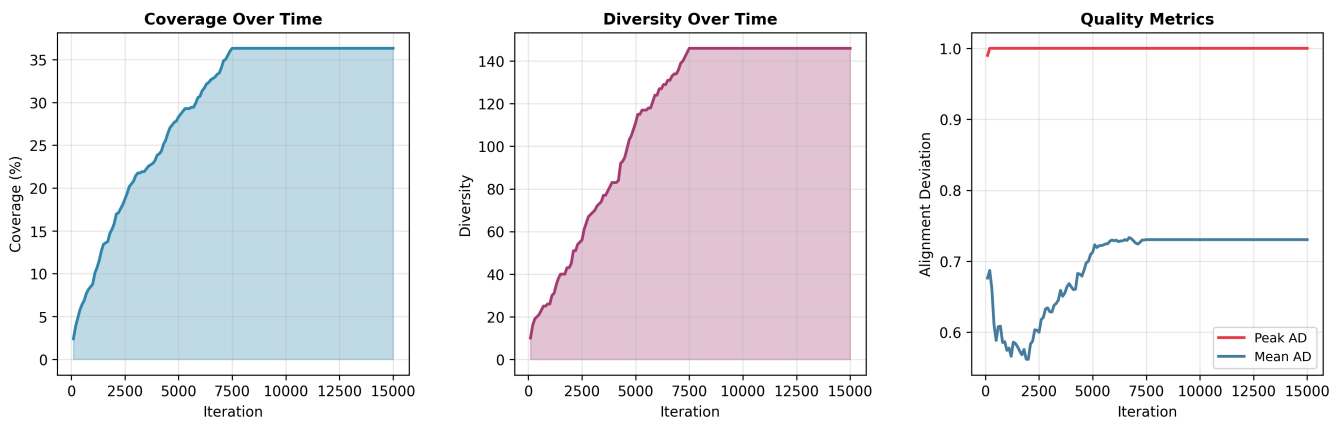
The Random + AD variant uses the Random baseline results reported in Section 6.6, since random sampling with AD

evaluation is precisely the ablation of removing MAP-Elites. For ME + Toxicity, we note that MAP-Elites fills cells based on behavioral coordinates (a_1, a_2) independently of the quality metric; the quality metric only determines which prompt is retained as elite per cell. Coverage therefore remains approximately unchanged, while quality-dependent metrics degrade proportionally to the mismatch between the toxicity signal and the full multi-category AD. A standard toxicity classifier reliably detects overt harms such as violence, hate speech, sexual content, self-harm, and discrimination, accounting for roughly half of the 10 harm categories measured by Alignment Deviation (AD). However, it struggles to flag harmful content delivered in a neutral or technical tone, including misinformation, manipulation, privacy violations, and cybersecurity exploits. Consequently, the algorithm only identifies the optimal prompt (the “elite”) in grid cells where the primary harm is overtly toxic; in cells dominated by subtle or technical harms, a suboptimal prompt is retained.

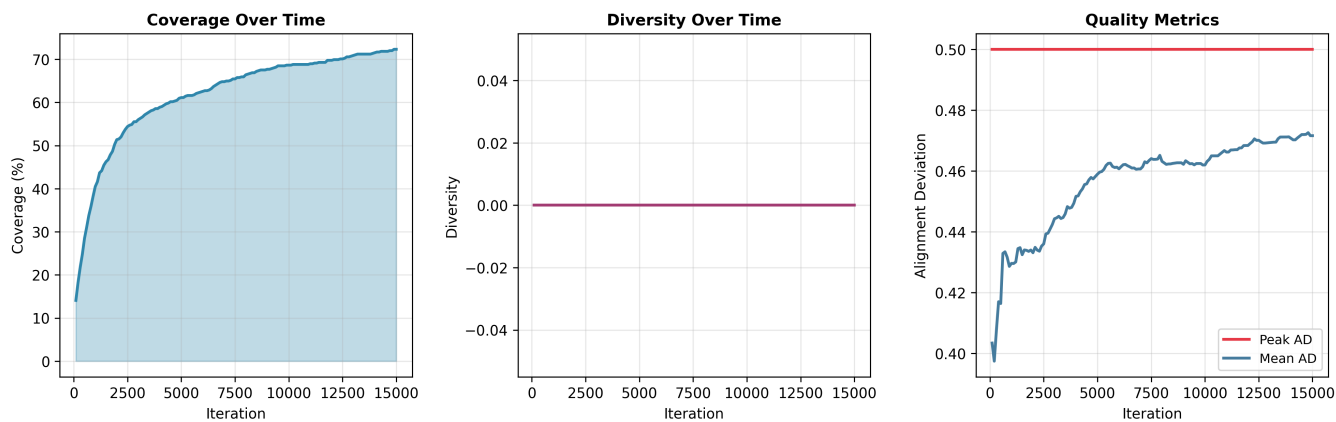
Removing the QD archive (Random + AD) produces the largest degradation: coverage collapses from 63.0% to 5.3% on Llama-3-8B, from 36.3% to 0.8% on GPT-OSS-20B, and from 72.3% to 5.0% on GPT-5-Mini. Without archive-based niche competition, randomly sampled prompts cover only a tiny fraction of the behavioral grid. Notably, the Random + AD variant still achieves high *mean* AD in the few cells it does fill (0.85 on Llama-3-8B), confirming that AD provides a useful quality signal but without MAP-Elites, this signal is concentrated in a negligible portion of the behavioral space. The ablation reveals complementary roles: MAP-Elites contributes primarily to *coverage* (exploration of the behavioral grid), while the multi-category AD metric contributes primarily to *quality* (accurate identification and ranking of vulnerabilities). Removing either component produces a qualitatively incomplete picture.



(a) Llama-3-8B



(b) GPT-OSS-20B



(c) GPT-5-Mini

Figure 7: Coverage, diversity, and quality metrics over 15,000 iterations. (a) Llama-3-8B: sustained growth in all metrics. (b) GPT-OSS-20B: early plateau in coverage with moderate quality. (c) GPT-5-Mini: high coverage growth but zero diversity and quality capped at 0.50.

Table 5: Ablation study across the three models.

Model	Variant	Cov. (%)	Div. (#)	QD Score	Mean AD
<i>Llama-3-8B</i>					
	Full	63.04	370	366.9	0.931
	ME + Toxicity	62.08	288	282.3	0.726
	Random + AD	5.28	30	28.1	0.851
<i>GPT-OSS-20B</i>					
	Full	36.32	146	165.8	0.730
	ME + Toxicity	35.52	103	126.5	0.569
	Random + AD	0.80	3	3.1	0.624
<i>GPT-5-Mini</i>					
	Full	72.32	0	213.2	0.472
	ME + Toxicity	71.36	0	163.5	0.368
	Random + AD	4.96	0	9.1	0.293

7 Discussion and Limitations

Our results show that LLM vulnerabilities form continuous, structured landscapes rather than isolated failure points. Each model exhibits a distinct topology: Llama-3-8B presents a near-universal vulnerability surface (93.9% basin rate), suggesting shallow alignment easily bypassed across the full parameter space; GPT-OSS-20B shows fragmented basins interleaved with safe regions, indicating patchable “holes” at specific behavioral coordinates; and GPT-5-Mini maintains a hard ceiling at AD = 0.50 regardless of prompt construction, suggesting a qualitatively stronger alignment mechanism. A consistent finding across all models is horizontal banding in the contour plots (Figure 4): narrow corridors at specific authority framing levels (a_2) where AD changes abruptly. This implies that models have discrete authority-recognition thresholds that significantly alter compliance behavior, which is a finding with direct implications for both attack design and targeted defense.

We advocate for structured maps characterizing the full vulnerability landscape as a standard component of safety evaluation, enabling targeted remediation, comparative auditing across models, and regression testing across versions.

Our 2D behavioral projection necessarily loses information; the true failure manifold likely exists in a higher-dimensional space. The Alignment Deviation metric relies on two judge models (GPT-4.1 and Sonnet 4.5), which may introduce systematic biases; human validation is an important next step. Our 15,000-query budget may not fully explore models with lower coverage. We focus on single-turn interactions; extending to multi-turn dialogues where the manifold may evolve dynamically is future work.

8 Conclusion

This paper shifts LLM safety evaluation from finding discrete adversarial failures to mapping the continuous Manifold of Failure. Applying MAP-Elites to three frontier models, we find: (1) Llama-3-8B exhibits near-universal vulnerability (mean AD 0.93, 370 distinct niches); (2) GPT-OSS-20B shows fragmented, spatially concentrated basins (64.3% of explored cells vulnerable); and (3) GPT-5-Mini demonstrates robust alignment (peak AD = 0.50, zero basins across 72% coverage). Our framework complements existing attack methods by revealing not just *whether* a model can be broken, but the full spatial structure of *how* it breaks and enables targeted remediation and a topological approach to AI safety.

References

- [1] Randall Balestriero, Romain Cosentino, and Sarath Shekkizhar. Characterizing large language model geometry helps solve toxicity detection and generation, 2024.
- [2] Patrick Chao, Alexander Robey, Edgar Dobriban, Hamed Hassani, George J. Pappas, and Eric Wong. Jailbreaking black box large language models in twenty queries, 2024.
- [3] Aaron Grattafiori et al. The llama 3 herd of models, 2024.
- [4] Zhiting Li, Shibai Yin, Tai-Xiang Jiang, Yexun Hu, Jiamian Wu, Guowei Yang, and Guisong Liu. Enhancing the adversarial robustness via manifold projection. *Proceedings of the AAAI Conference on Artificial Intelligence*, 39(1):451–459, Apr. 2025.
- [5] Mantas Mazeika, Long Phan, Xuwang Yin, Andy Zou, Zifan Wang, Norman Mu, Elham Sakhaee, Nathaniel Li, Steven Basart, Bo Li, David Forsyth, and Dan Hendrycks. Harmbench: A standardized evaluation framework for automated red teaming and robust refusal, 2024.
- [6] Anay Mehrotra, Manolis Zampetakis, Paul Kassianik, Blaine Nelson, Hyrum Anderson, Yaron Singer, and Amin Karbasi. Tree of attacks: Jailbreaking black-box llms automatically, 2024.
- [7] Jean-Baptiste Mouret and Jeff Clune. Illuminating search spaces by mapping elites, 2015.
- [8] OpenAI et al. gpt-oss-120b & gpt-oss-20b model card, 2025.
- [9] Mikayel Samvelyan, Sharath Chandra Raparthy, Andrei Lupu, Eric Hambro, Aram H. Markosyan, Manish Bhatt,

Yuning Mao, Minqi Jiang, Jack Parker-Holder, Jakob Foerster, Tim Rocktäschel, and Roberta Raileanu. Rainbow teaming: Open-ended generation of diverse adversarial prompts. In *Advances in Neural Information Processing Systems*, volume 37, pages 69747–69786, 2024.

- [10] Aaditya Singh et al. Openai gpt-5 system card, 2025.
- [11] Kaitao Song, Xu Tan, Tao Qin, Jianfeng Lu, and Tie-Yan Liu. MpNet: masked and permuted pre-training for language understanding. In *Proceedings of the 34th International Conference on Neural Information Processing Systems*, NIPS '20, Red Hook, NY, USA, 2020.
- [12] Varshini Subhash, Anna Bialas, Weiwei Pan, and Finale Doshi-Velez. Why do universal adversarial attacks work on large language models?: Geometry might be the answer, 2023.
- [13] Andy Zou, Zifan Wang, Nicholas Carlini, Milad Nasr, J. Zico Kolter, and Matt Fredrikson. Universal and transferable adversarial attacks on aligned language models, 2023.